

Symmetry Reduced Exact Coherent Structures in Plane Couette Flow

A Thesis
Presented to
The Division of Mathematics and Natural Sciences
Reed College

In Partial Fulfillment
of the Requirements for the Degree
Bachelor of Arts

Varchas Gopalaswamy

March 28, 2015

Approved for the Division
(Physics)

Daniel Borrero

Introduction

I am an old man now, and when I die and go to heaven, there are two matters on which I hope for enlightenment. One is quantum electrodynamics, and the other is the turbulent motion of fluids. And about the former, I am optimistic

Horace Lamb, 1932

The turbulence problem can be stated simply – Is there a predictive model for the development of the internal structures of turbulent flows? In this case it is deceptively simple, for much like a small, unnamed village in coastal Armorica holding out against the Romans, the turbulence problem that has confounded physicists and engineers for centuries. Understanding turbulence is vitally important, since turbulent flows appear in artificial scenarios such as the flow around ships or aircraft, and in natural scenarios from the atmosphere of Jupiter to the blood flow in the heart. Turbulent flows are typically characterized by the **Reynolds number**, which is the (dimensionless) ratio between the inertial and viscous damping forces. At small Re , viscosity dominates, and smooths out large velocity gradients in the fluid, resulting in the well-ordered **laminar** flow. At large Re , kinetic energy is dissipated at a lower rate, allowing for the existence of increasingly complex flow structures, such as eddies or vortices, which are characteristic of turbulence.

Transition to Turbulence

From the definition of the Reynolds number, it is clear that in the limit of $Re \rightarrow 0$, the only steady state solution is the laminar flow state, while in the limit $Re \rightarrow \infty$, turbulent flow states can also exist. It might therefore be reasonable to expect that as Re increases, the flow should become steadily more turbulent. However, experiments in Taylor-Couette and pipe flows, among others, indicate that turbulence develops suddenly at some critical value of Re . There are in general two routes by which systems transition to turbulence. In the supercritical transition, an increase in Re above some critical value results in the loss of global stability of the laminar state¹ and the

¹That is to say, it is no longer stable against perturbations of any amplitude

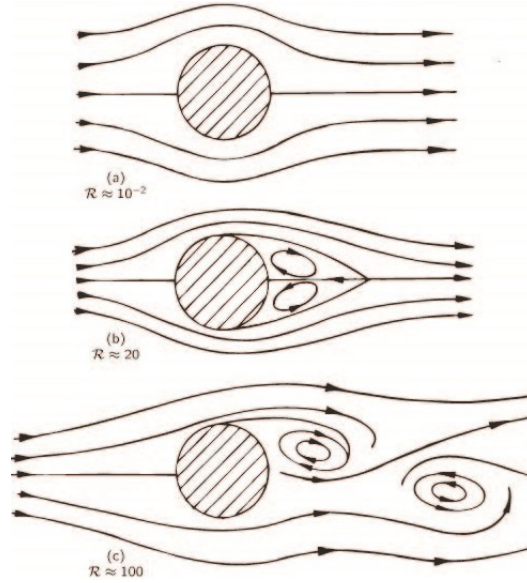


Figure 1: Representations of cylinder wakes at various Re . Notice that the flow goes from laminar in (a) to turbulent in (c), with two prominent vortices. Reproduced from the Feynman Lectures on Physics, Chapter 41.

emergence of new stable solutions of higher complexity, which eventually bifurcate into even more complex states at higher critical values, eventually resulting in turbulence. Supercritical transitions occur in Taylor-Couette flow with low outer-cylinder rotation rates, and well as in Rayleigh-Bernard convection.

The second, more complex transition is the subcritical transition. In the subcritical transition, the laminar state loses global stability at lower Re than linear stability analysis would predict, and the flow transitions *directly* to turbulence, instead of increasingly steadily in complexity. Since they are not well predicted by linear stability analysis, subcritical transitions are less well understood, but nevertheless can be physically important. Subcritical transitions occur in pressure-driven flows in pipes, which models flows such as those in hypodermic needles or lung alveoli, or shear-driven flow between two infinite parallel plates (displayed in Figure 2), which is known as plane Couette flow, and is the focus of this thesis [4, 15].

Plane Couette Flow

The geometry of the full plane Couette system is extremely simple, with only one geometrical parameter h , the half-distance between the parallel plates, and one kinematic parameter V , the velocity of the upper plate², giving the Reynolds number

²While in principle the upper and lower plate can have different velocities, there should always be a reference frame in which the upper plate has velocity V , and the lower plate has velocity $-V$.

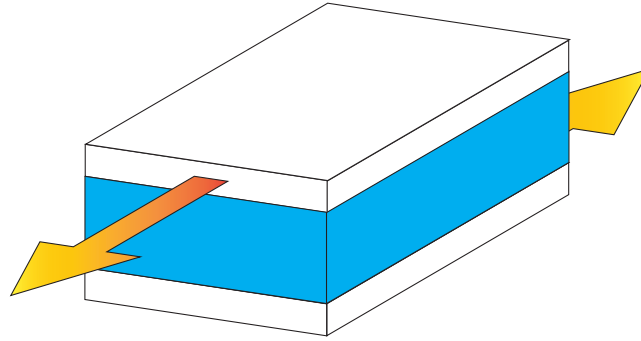


Figure 2: A diagram of the plane Couette geometry. The upper and lower plates extend infinitely in the plane, as does the fluid filling the gap.

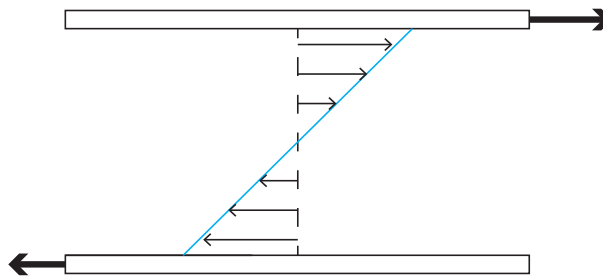


Figure 3: A cross-sectional representation of plane Couette flow, with the laminar velocity profile shown. By symmetry, the laminar profile must be the same everywhere.

as

$$Re = \frac{hV}{\nu}, \quad (1)$$

where ν is the kinematic viscosity. When Re is very small, only the laminar flow state is stable, which in the case of plane Couette flow is given by the linear velocity profile shown in Figure 3. As Re increases, however, we would expect the emergence of long lived turbulence, which has been seen in experiments [3].

Tackling Turbulence

The traditional approach towards the analysis of turbulence for the last century has been the statistical approach initially developed by Reynolds, Prandtl, von Karman, Kolmogorov and others [17]. At the core of the statistical approach to turbulence is the assumption that turbulent flow states can be expressed as random perturbations around some mean flow. At extremely high Re , where direct numerical simulation (DNS) of the flow is computationally infeasible, the statistical approach is invaluable, but at low-to-moderate Re , these models can become less accurate – for example, Reynolds stress models have no Re dependence, but DNS shows that there are Re -dependent effects. Even ignoring the moderate Re behavior of the statistical models, the fundamental issue with the statistical approach is its discarding of the dynamical information about turbulence. Methods like RANS time average the perturbations

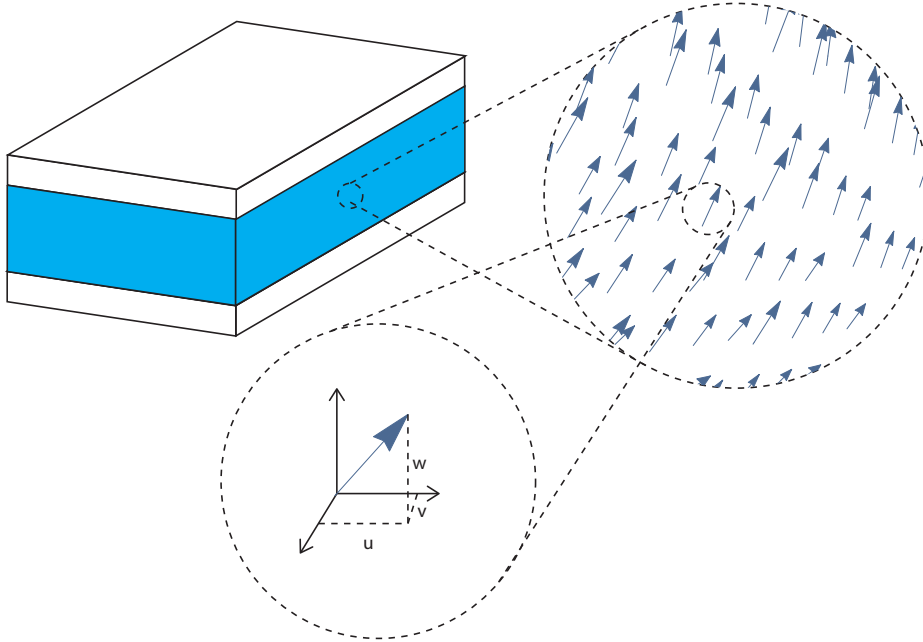


Figure 4: At each point in the fluid volume, the velocity field has a value that is described by three numbers, thus requiring three dimensions to track over time.

away, while LES explicitly does not resolve small scale structures, and thus cannot truly provide an answer to the turbulence problem.

An alternate approach was proposed by Eberhard Hopf in 1948. Hopf suggested that solutions to the Navier-Stokes equations might be thought of as trajectories in an infinite dimensional state space in which each point corresponded to a possible velocity field. To better understand what this would mean, consider the velocity field at a point in the fluid, pictured in Figure 4. In order to describe the velocity vector, three numbers are required (each of which can take any real value), so this microsystem has three dimensions. Now any finite fluid volume will have an uncountably infinite number of points at which the velocity field has a value, so we would need an uncountably infinite set of numbers to describe any velocity field, which would then reside in an infinite dimensional vector space. Luckily, every point in the space does not necessarily correspond to a solution of the Navier-Stokes equation; for finite Re , for instance, the gradient of the velocity field cannot be too large. Hopf thus conjectured that physical trajectories, corresponding to solutions to the Navier-Stokes equation would lie on some finite-dimensional manifold (known as the **inertial manifold**) embedded within this infinite dimensional space. This transition of an inertial manifold from infinite to finite dimensional spaces by varying a control parameter has been rigorously demonstrated under certain conditions [6]. For the Navier-Stokes equation, the inertial manifold's control parameter is Re , and physical intuition suggests that its structure should also have Re dependence, since at very low Re , the only physical solution is the laminar state, and as Re increases, more complex flows become physically permissible. Hopf proposed finally that turbulence in this view

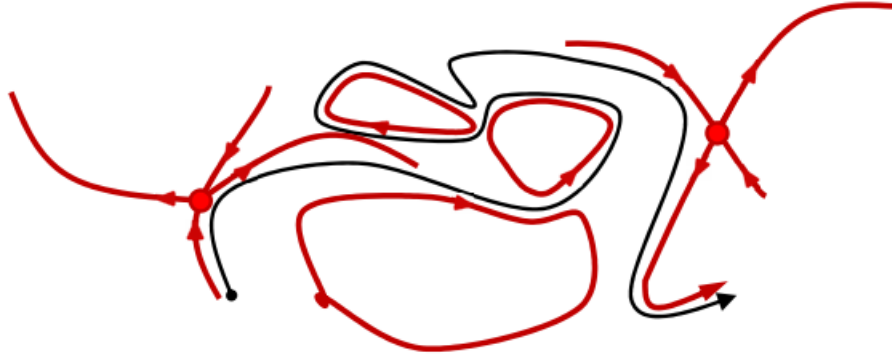


Figure 5: A turbulent trajectory in black appears chaotic in isolation, but is in fact guided by exact coherent structures of the flow

was simply a trajectory that would travel across wide distances on the manifold.

Unfortunately for Hopf, the computer power necessary to pursue this line of work was not available in 1948, leading him to comment in frustration that “the great mathematical difficulties of these important problems are well known and at present the way to a successful attack on them seems hopelessly barred”. It would take until 1963 and the derivation of the Lorenz attractor for the first numerical state-space analysis of turbulence [14], albeit for a highly truncated version of Navier-Stokes, designed to investigate Rayleigh-Bernard convection. There have also been a number of efforts to explore the structure of invariant manifolds in moderate turbulence Navier-Stokes, such as Proper Orthogonal Decomposition [1] and the ‘self-sustaining process theory’ [2], but while fruitful they are nevertheless models of turbulent flow, and not an exact analysis of Navier-Stokes. Another avenue of research emerged in 1990, when Nagata computed nontrivial equilibrium flow states in plane Couette flow by continuing the wave vortex solution of Taylor-Couette flow [16]. This class of solutions, which were named **exact coherent structures** by Waleffe [19] are the result of calculating exact, invariant solutions of the fully resolved Navier-Stokes equation. The family of exact coherent structures was expanded with the discovery of travelling wave equilibria by Nagata in 1997, the computation of periodic orbits by Kawahara and Kida in 2001 [12], and the computation of *relative* periodic orbits³ by Viswanath in 2007 [18]. The ultimate hope of this line of research is that turbulence can be viewed as chaotic trajectories on the inertial manifold that are guided by exact coherent structures (Figure 5), implying that a fundamental understanding of exact coherent structures would lead to a better understanding of turbulent dynamics.

While there has been a great deal of progress in this field, much of it has been computational, though experiments by Hof and de Lozar are at present the only direct experimental verifications for the existence of exact coherent structures in nature. However, indirect results, such as the resemblance of the upper branch solution to the

³That is, flow states that are periodic after some phase shift

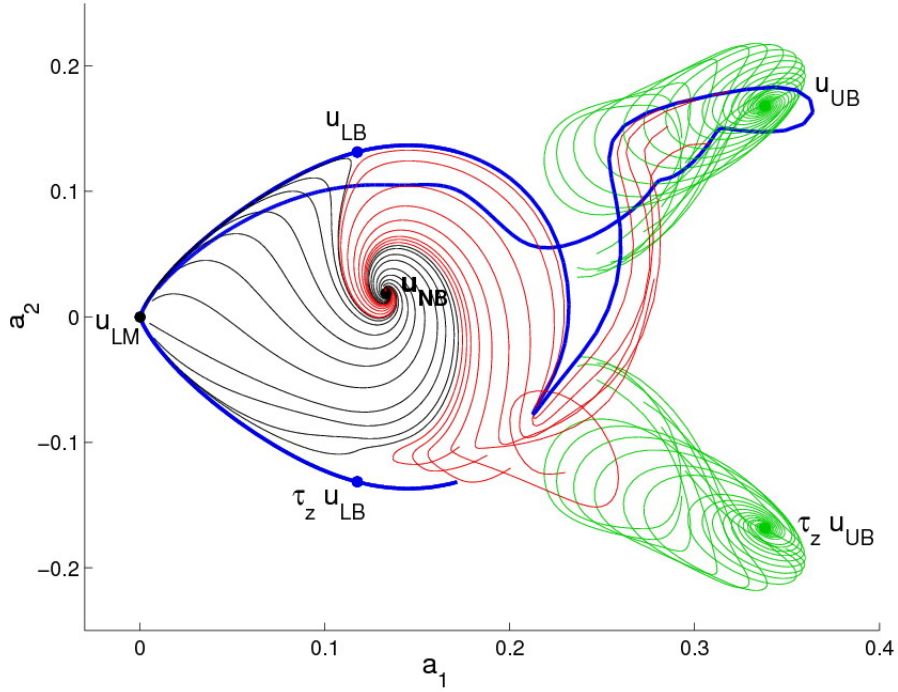


Figure 6: A 2D projection of the upper, lower and newbie branch solutions. The area in between the UB and LB solutions and their symmetric translations is the area of interest. Adapted from [8]

roll-streak structure seen in DNS [8], and the potential role of the stable manifold of the lower branch solution in separating the turbulent and laminar basins of attraction suggest that exact coherent structures likely play a fundamental role in the behavior and evolution of turbulent flow states. Advances in computing power, along with the development of CFD algorithms such as Channelflow [7] have also made the computation of these structures generally feasible, and allow for the investigation of reduced symmetry exact coherent structures. In order to compute the original exact coherent structures, substantial symmetry constraints were placed upon the dynamics. This had the benefit of greatly reduced computational complexity, but resulted in exact coherent structures that flanked the turbulent basin of attraction. While these structures can provide insight into turbulent transitions, they cannot provide a great deal of insight into trajectories within the turbulent basin.

Chapter 1

Equations of Flow

For every action, there is an equal
and opposite regulatory body

Anonymous

1.1 Formalisms

If we were considering the dynamics of a point particle, we would begin with Newton's Second Law -

$$\frac{d\mathbf{p}}{dt} = \mathbf{F}, \quad (1.1)$$

write down the body force as a function of position, time, etc., and have our differential equation, whose solution may be analytic or numeric, but is nevertheless trivial. While we can in principle use this approach to describe the behavior of a large collection of particles making up the fluid, practical considerations prevent us from modelling the behavior of each individual particle, for the following reason – in a milliliter of water, there are approximately 10^{22} molecules of water, each with 6 degrees of freedom¹. Applying (1.1) to all these particles would result in about 10^{23} coupled partial differential equations. Such a set of equations would be hard to write down, let alone solve! Clearly, a more intelligent approach is needed.

1.1.1 The Eulerian Formulation

When asked to consider the mechanical evolution of some collection of bodies, two obvious methods would be readily apparent - we could either follow a collection of particles on their way through space and time (the **Lagrangian** formulation), or we could situate ourselves at some point in space and observe the properties of particles that pass through the surrounding region (the **control volume**) over time

¹If we ignore the vibrations of the O-H bond

(the **Eulerian** formulation). The Lagrangian formulation will be familiar to anyone with a basic physics education, since it lends itself readily towards analysis of rigid-body motion. When considering fluids, however, the disadvantages of the Lagrangian formulation (noted above) stand in contrast to the ease of analysis afforded by the Eulerian formulation, which remains as easy (or hard) as it was for rigid body motion. For this reason, I will focus on the Eulerian formulation of fluid mechanics in this thesis.

1.1.2 The Fluid Particle

As a consequence of the Eulerian formulation, we cannot know the full timeline of any individual particle over its lifetime – we only know the properties of particles within the control volume. As a result, the principle quantity of consideration for the Eulerian formulation is therefore the velocity field² $\mathbf{v}(\mathbf{x}, t) = v_x(\mathbf{x}, t)\hat{\mathbf{x}} + v_y(\mathbf{x}, t)\hat{\mathbf{y}} + v_z(\mathbf{x}, t)\hat{\mathbf{z}}$, along with the pressure and density fields, which are the average values of the property in a control volume surrounding a point. A subtle issue arises in doing this, however. Since the velocity field is continuous, it has a well defined value at every point in space, which we would want to be associated with the velocity of a particle at that point in space. But there are finite number of particles in any collection of fluid with a finite spatial extent - so it would appear that the formulation assigns multiple different velocities to a single particle! The resolution to this is the continuum hypothesis, which suggests that the control volume (the ‘**fluid parcel**’) can be chosen such that it is large enough to form a meaningful average of the quantities within, but small enough that the properties do not vary significantly over the parcel, and that from a macroscopic perspective, the properties appear continuous. Can such a parcel even exist? As an example, let us consider water, with approximately 10^{22} atoms per cubic centimeter. Imagine our fluid parcels as cubes filling up space, with sides of length dl , giving a total volume of dl^3 . First, let us make dl small enough that the macroscopic properties appear continuous - how about one micron? That gives the volume of a fluid particle as one cubic micrometer. For scale, consider that the volume of the human red blood cell ranges from 80-100 cubic micrometers[5] - this seems acceptably small for considering, say, the flow around a ship.³ The number of water molecules within each fluid parcel is then

$$10^{22}dl^3 = 10^{22} \times 10^{-12} = 10^{10}, \quad (1.2)$$

or about 10 billion water molecules, which is certainly sufficient to achieve a meaningful average. Having defined a fluid parcel in this way allows us to behave as if these external variables have well defined values at every point in space, which greatly simplifies the following analysis.

²As opposed to particle trajectories $\mathbf{x}(t)$ in the Lagrangian formulation.

³The validity of the continuum hypothesis is clearly dependent on the density of the fluid and the length scale of the phenomenon to be modelled, but holds up even for the sparse gas clouds of protoplanetary disks

1.2 Mass Conservation

While not technically a part of the Navier-Stokes equation (which is a statement about conservation of linear momentum), conservation of mass is nevertheless essential in solving fluid problems, and will serve as an easy demonstration of the control volume principle. Consider a volume Ω which is fixed in space, and has some mass density $\rho = \rho(\mathbf{x}, t)$ and some fluid velocity $\mathbf{v} = \mathbf{v}(\mathbf{x}, t)$ that are generically functions of time and space, allowing us to define the **mass current density** $\mathbf{m} = \mathbf{v}\rho$. We would prefer that our equations do not allow mass to disappear (excluding high-energy physics, naturally), and would additionally prefer a mathematical form of this statement.

The mass contained within the volume is given by

$$M = \int_{\Omega} \rho \, dV, \quad (1.3)$$

the flow of mass out of the volume through the surface $d\Omega$ of Ω is given by

$$M_{flow} = \int_{d\Omega} \mathbf{m} \cdot \mathbf{n} \, dA = \int_{\Omega} \nabla \cdot (\rho \mathbf{v}) \, dV, \quad (1.4)$$

by the divergence theorem. Now if mass is conserved, the sum of the rate of mass flow into (or out of) the volume and the rate of change of mass inside the volume must be zero, giving

$$\frac{\partial M_{encl}}{\partial t} + M_{flow} = 0, \quad (1.5)$$

$$\frac{\partial}{\partial t} \left(\int_{\Omega} \rho \, dV \right) + \int_{\Omega} \nabla \cdot (\rho \mathbf{v}) \, dV = 0, \quad (1.6)$$

but since Ω is time independent, the time derivative commutes with the integral, giving

$$\int_{\Omega} \frac{\partial \rho}{\partial t} + \nabla \cdot (\rho \mathbf{v}) \, dV = 0, \quad (1.7)$$

but since Ω is arbitrary, the integrand must be zero everywhere, giving the statement of conservation of mass in differential form:

$$\frac{\partial \rho}{\partial t} + \nabla \cdot (\rho \mathbf{v}) = 0. \quad (1.8)$$

Now, (1.8) can be expanded further by using the chain rule for divergence, giving

$$\frac{\partial \rho}{\partial t} + \rho \nabla \cdot \mathbf{v} + \mathbf{v} \cdot \nabla \rho = 0. \quad (1.9)$$

If the flow is (approximately) incompressible, which will be true for small Mach numbers⁴, then ρ must be constant, and (1.9) becomes

$$\nabla \cdot \mathbf{v} = 0, \quad (1.10)$$

for both steady and unsteady flows.

⁴The Mach number is the ratio of the fluid velocity to the speed of sound in the fluid. v_{sound} for water is 1497 ms^{-1} at room temperature and pressure.

1.3 Conservation of Linear Momentum

As mentioned earlier, the Navier-Stokes equations are simply a statement of conservation of linear momentum, along with certain assumptions about stress (an object that contains information about forces) and strain (an object that contains information about how the fluid deforms in response to the applied forces), which are presented below.

1.3.1 Stress

For a control volume Ω with boundary $d\Omega$, there are in general three ways in which momentum can be change over time in Ω by transport through $d\Omega$ (i.e., forces on $d\Omega$):

1. Bulk, ‘convective’ flow across $d\Omega$
2. Surface-normal transfer through elastic collisions between molecules. This is the microscopic origin of pressure.
3. Transfer through stochastic motion of molecules through $d\Omega$, as in Figure ??.
Since it is stochastic, time-averaged mass does not change, but momentum can still be transferred. This leads to viscous stresses, and can be both normal and tangential (shear).

We define positive stress as stress that acts towards the control volume, and negative if they act away. Now, a stress on a fluid volume is not quite a vector, like force. Not only does it have a magnitude and direction, but it also has a plane that it acts from. Since there are three directions and three planes of action, stress objects generally have nine elements, and is a **second rank tensor**. That is, the viscous stress tensor \mathcal{T} is identified by two subscripts, where the first subscript indicates the plane of action, and the second the direction of action. So \mathcal{T}_{xy} would represent the viscous force on the (y, z) plane acting in the y direction. Note than in a Cartesian coordinate system, a second rank tensor can be written as a matrix.

1.3.2 Strain

Now that we can consider the forces on a fluid particle, we need to link these forces back to our external variables. In solids, this is easy - Hooke’s Law, for instance, sets the strain proportional to the stress:

$$\sigma = \mathcal{C}\epsilon, \tag{1.11}$$

where σ is the Cauchy stress tensor, \mathcal{C} is the (fourth rank) stiffness tensor and ϵ is the infinitesimal strain tensor. However, for fluids, this is not the case - you can imagine that if you applied a constant force to a cube of water, it would deform continuously, without offering any resistance. Newton theorized that for continuously deformable

fluids, the 1-D relationship between stress \mathcal{T} and strain \mathcal{S} should have the following form:

$$\mu \frac{d\mathcal{S}}{dt} = \mu \frac{du}{dx} = \mathcal{T}, \quad (1.12)$$

where μ is the viscosity and u is the velocity. Stokes extended this to three dimensions, giving the Newtonian constitutive relationship between stress and strain (for an incompressible fluid):

$$\mathcal{T}_{ij} = -p\delta_{ij} + \mu \left(\frac{\partial u_i}{\partial x_j} + \frac{\partial u_j}{\partial x_i} \right), \quad (1.13)$$

where δ_{ij} is the Kronecker delta function. Water, and most gases under normal conditions are Newtonian, but fluids like blood, quicksand and corn starch (to name a few) are not.

1.3.3 Surface Forces

Having written down the stress tensor \mathcal{T} as a function of the velocity field, we now link it to the surface forces on a fluid particle. Recalling that stresses act over $d\Omega$ of the fluid particle, the total force is then simply

$$\mathbf{F} = \int_{d\Omega} \mathcal{T} \cdot \mathbf{n} \, dA, \quad (1.14)$$

where \mathbf{n} is the surface normal.

1.3.4 Newton's Second Law

For a fluid parcel Ω , Newton's Second Law can be rewritten as

$$\sum \mathbf{F} = \int_{\Omega} \frac{\partial \mathbf{p}}{\partial t} \, dV \quad (1.15)$$

where the sum is over all possible external forces. We can further split \mathbf{F} into two kinds of forces - body forces, like gravity or electromagnetism, and surface forces due to stress. We group the body forces \mathbf{F}_b as

$$\mathbf{F}_b = \int_{\Omega} \rho \mathbf{f} \, dV, \quad (1.16)$$

where \mathbf{f} is the **body force density**. Using (1.14) to express the surface forces, Newton's Second Law becomes

$$\int_{\Omega} \rho \mathbf{f} - \frac{\partial \mathbf{p}}{\partial t} \, dV + \int_{d\Omega} \mathcal{T} \cdot \mathbf{n} \, dA = 0, \quad (1.17)$$

which can be written in differential form by the same trick used to generate (1.8), giving Cauchy's Equation of Motion

$$\rho \mathbf{f} - \frac{\partial \mathbf{p}}{\partial t} + \nabla \cdot \mathcal{T} = 0. \quad (1.18)$$

From this, the incompressible Navier-Stokes equation arise by a substitution of (1.13) into (1.18), giving (after tedious rearrangement by components),

$$\frac{\partial \mathbf{V}}{\partial t} + (\mathbf{V} \cdot \nabla) \mathbf{V} = \mathbf{f} - \frac{1}{\rho} \nabla p + \frac{\mu}{\rho} \nabla^2 \mathbf{V}. \quad (1.19)$$

By using the substitutions

$$\mathbf{x} \Rightarrow L\mathbf{s} \quad (1.20)$$

$$\mathbf{V} \Rightarrow U\mathbf{u} \quad (1.21)$$

$$t \Rightarrow \frac{L}{U}\tau \quad (1.22)$$

$$p \Rightarrow \rho U^2 p', \quad (1.23)$$

and neglecting body forces, we obtain the nondimensional version of (1.19) –

$$\frac{\partial \mathbf{u}}{\partial \tau} + (\mathbf{u} \cdot \nabla) \mathbf{u} = -\nabla p' + \frac{1}{Re} \nabla^2 \mathbf{u}, \quad (1.24)$$

where

$$Re = \frac{UL\rho}{\mu}. \quad (1.25)$$

. In practice, the values of L and U are chosen by convention to reflect the natural scales of the problem at hand.

1.4 Plane Couette Flow

The Navier-Stokes equation for plane Couette flow is given by

$$\frac{\partial \mathbf{u}}{\partial \tau} + (\mathbf{u} \cdot \nabla) \mathbf{u} = \frac{1}{Re} \nabla^2 \mathbf{u}, \quad (1.26)$$

with geometry as pictured in Figure 2. We nondimensionalize by the velocity of either plate and the half-plate distance, with the Reynolds number then defined as in (1.25). Since plane Couette flow is a shear driven flow, we set the pressure gradient to zero, with no slip boundary conditions at the walls. In order to derive the laminar velocity profile shown earlier in Figure 3, note that at very low Re , the left hand side of (1.26) dominates. If we assume that the flow is unidirectional and steady, so that $\mathbf{u} = u_x \hat{\mathbf{x}}$, and since by symmetry considerations the velocity field can only be a function of height, the Navier-Stokes equation reduces to

$$\frac{\partial^2 u_x}{\partial y^2} = 0, \quad (1.27)$$

with no-slip boundary conditions

$$u(-1) = -1, \quad (1.28)$$

$$u(1) = 1, \quad (1.29)$$

which gives the linear laminar flow profile

$$\mathbf{u}(y) = y\hat{\mathbf{x}}. \quad (1.30)$$

Consider then a perturbation $\mathbf{v}(x, y, z, t)$ from this laminar state, so that the initial field is $\mathbf{u}(x, y, z, t) = \mathbf{v}(x, y, z, t) + y\hat{\mathbf{x}}$. Substituting this into (1.24), we get

$$\frac{\partial \mathbf{v}}{\partial \tau} + y \frac{\partial \mathbf{v}}{\partial x} + v\hat{\mathbf{x}} + \mathbf{v} \cdot \nabla \mathbf{v} = \frac{1}{Re} \nabla^2 \mathbf{v}, \quad (1.31)$$

$$\nabla \cdot \mathbf{v} = 0, \quad (1.32)$$

with boundary conditions

$$\mathbf{v}(x, \pm 1, z, t) = 0 \quad (1.33)$$

as the equation of motion for the perturbing velocity field. Since the laminar profile is steady, understanding the turbulent field's trajectory in state space now reduces to understanding the behavior of the turbulent perturbation, and the structure of its inertial manifold.

Chapter 2

Symmetry in plane Couette flow

Tyger! Tyger! burning bright,
In the forests of the night.
What immortal hand or eye,
Could frame thy fearful symmetry?

William Blake, *The Tyger*

Dynamical systems in physics often display symmetry. The electron wavefunction in hydrogen, or the gravitational motion of a planet around a star, for instance, display very high degrees of spatial symmetry. Understanding the symmetries of a system can be incredibly useful to an investigator, since they hint at conserved physical quantities (through Noether's Theorem), and can greatly reduce the complexity of the system in various ways¹. Before I begin the discussion of the symmetries of plane Couette flow, I will first define what 'symmetry' means in this thesis. A system is said to be **equivariant** under a symmetric transformation of the dynamical system if a transformation that commutes with the time evolution of the system - that is, for a symmetric transformation S and a dynamical system $\dot{x} = f(x)$, $S\dot{x} = Sf(x) = f(Sx)$ implies that the system is equivariant under S .

The symmetry relations of plane Couette flow have been derived extensively in [9], which I will present here for the sake of flow².

2.1 Unbounded Navier-Stokes

If we do not impose boundary conditions on the Navier-Stokes equations on an infinite domain, the system will be equivariant under continuous rotational and translational symmetry, as well as the discrete **pointwise inversion** symmetry σ_{xz} , which has the following action on the system:

¹In quantum mechanics, for instance, symmetries in the Hamiltonian imply the existence of operators that commute with it, which can allow one to greatly simplify the Hamiltonian matrix via simultaneous diagonalization for computational problems

²haha

$$\sigma_{xz} \mathbf{u}(\mathbf{x}) = -\mathbf{u}(-\mathbf{x}) \quad (2.1)$$

While the rotation or translation transformation can be easily conceptualized, the pointwise inversion can provide some difficulty. The easiest way of visualizing the transformation is to view it in a 2D domain instead of in the full 3D, as shown in Figure ?? . The proof of the equivariance of these transformations can be found in [?].

2.2 Plane Couette Flow

If the domain is limited to $\mathbb{R}^2 \times [-1, 1]$ with the boundary conditions of plane Couette flow, we lose some of the equivariant transformations of the full, unrestricted problem, leaving us with two basic discrete symmetries: a rotation by π about the z axis (denoted σ_x and a reflection about the z axis (denoted σ_z)³, with together form a discrete symmetry group $D = D_1 \times D_1 = \{e, \sigma_x, \sigma_z, \sigma_{xz}\}$ of order 4, where

$$\sigma_x[u, v, w](x, y, z) = [-u, -v, w](-x, -y, z) \quad (2.2)$$

$$\sigma_z[u, v, w](x, y, z) = [u, v, -w](x, y, -z) \quad (2.3)$$

$$\sigma_{xz}[u, v, w](x, y, z) = [-u, -v, -w](-x, -y, -z) \quad (2.4)$$

The continuous symmetries are the two parameter streamwise-spanwise translations, which, when provided periodic boundary conditions, form a continuous $SO(2) \times SO(2)$ symmetry group

$$\tau(l_x, l_z)[u, v, w](x, y, z) = [u, v, w](x + l_x, y, z + l_z). \quad (2.5)$$

The group Γ of equivariant solutions is then any combination of these symmetry operations, given by $\Gamma = SO(2)_x \ltimes D_{1,x} \times SO(2)_z \ltimes D_{1,z}$ ⁴. For a solution \mathbf{u} of plane Couette flow, the group s of symmetries that satisfies $s\mathbf{u} = \mathbf{u}$ is called the isotropy subgroup of \mathbf{u} and is said to fix \mathbf{u} . Examples of such groups include the identity group $\{e\}$, which is typically the isotropy subgroup of turbulent solutions. Before I discuss the isotropy subgroup considered for this thesis, however, I will first highlight the useful properties of some particular symmetry subgroups to motivate the eventual choice of isotropy subgroup.

2.3 Properties of Γ

It should be evident that since plane Couette flow is equivariant under the continuous translations given in (2.5), trajectories can be traveling wave equilibria or relative periodic orbits: that is, if one moves into a different inertial frame, the trajectory is a

³The motivation for these subscripts will become apparent shortly

⁴ \ltimes is the semidirect product

regular equilibrium or periodic orbit. However, an initial condition that is fixed by σ_z cannot be translated in the spanwise direction without losing σ_z symmetry (except for the trivial case where $\frac{\partial \mathbf{u}_z}{\partial z} = 0$). Similarly, an initial condition that is fixed by σ_x cannot be translated in the streamwise direction without losing σ_x symmetry (and an initial condition that is fixed by σ_{xz} symmetry cannot be translated at all without losing σ_{xz} symmetry). Since these symmetries are also invariant⁵, a trajectory with one of the discrete symmetries cannot have traveling waves in the direction corresponding to its subscript.

The presence of the periodic boundary conditions also implies that all solutions are fixed by the full-period translation $\tau(L_x, 0)$ and $\tau(0, L_z)$. However, solutions can also be fixed by any rational translation of the form $\tau(\frac{m}{n}L_x, \frac{m'}{n'}L_z)$, or by the continuous translations. In the latter case, the velocity field is necessarily constant along the translation direction, but in the former, it implies that the periodic cell is subdivided into repeating subcells. In this case, we can simply reduce the domain to the subcell, which implies that we need not fix \mathbf{u} under any translational symmetry other than the full period relation, which is required by the boundary conditions.

Finally, we can reduce the number of unique subgroups of Γ by considering its **conjugacy groups**. A group N and M are considered conjugate if for some $s \in \Gamma$, $N = s^{-1}Ms$ - that is, N and M are related by a coordinate transformation. This allows us to consider only one group out of a set of mutually conjugate groups (known as a conjugacy class), since any other group in the class is simply related by the application of a symmetry transformation. This becomes especially important when considering $O(2) = SO(2) \ltimes D_1$, since it is not an abelian group as reflections and translations about the same axis are noncommutative (Figure ??). However, we can still recover a psuedo-commutative relation by considering Figure ?. We can see that $\sigma_z\tau_z$ results in the object moving by l_z to the right, and the being mirrored across the z axis, at which point it is mirrored and l_z to the left of the origin. We can achieve the same effect by mirroring the object and moving it to the left - that is, applying the operation $\tau_z^{-1}\sigma_z$, leading us to conclude that $\sigma\tau = \tau^{-1}\sigma$. We can rewrite this as $\sigma\tau^2 = \tau^{-1}\sigma\tau$, so

$$\sigma_x\tau(l_x, 0) = \tau^{-1}(l_x/2, 0)\sigma_x\tau(l_x/2, 0), \quad (2.6)$$

which implies that σ_x and $\sigma_x\tau_x$ are part of the same conjugacy class - so if a isotropy group contains $\sigma_x\tau_x$, there is a simpler version of that group which contains σ_x instead. Note that if $l_x = L_x$, then we have $\sigma_x = \tau_x^{-1}\sigma_X\tau_x$, so reflection and translations commute for any half-integer cell shifts. In this thesis, I will work with either half-cell or or null shifts. The group of half cell shifts is denoted C_2 , so the group

$$G = D_{1,x} \times C_{2,x} \times D_{1,z} \times C_{2,z} \subset \Gamma \quad (2.7)$$

⁵That is, if the symmetry is satisfied at time $t = t_0$, it must be satisfied for all times.

is an abelian group of order 16, containing both the isotropy groups of half-cell and null shifts.

2.4 Symmetry Groups of this Thesis

We can categorize the conjugacy classes of G by their order - in this thesis, we will work with order 2 and 4 classes. There are 15 subgroups of order-2 (since there are 15 non-identity elements in G), 35 subgroups of order 4 $((15 \cdot 14)/(3 \cdot 2))$, 15 subgroups of order 8 and 1 subgroup of order 16, giving 67 subgroups of G . Luckily, the existence of conjugacy classes allow us to greatly simplify the number of distinct groups we need to consider. For order-2 subgroups, conjugacy between σ_x and $\sigma_x\tau_x$ and $\sigma_z\tau_z$ allows us to simplify down to just 8 distinct groups, which are generated by $\sigma_x, \sigma_z, \sigma_{xz}, \sigma_x\tau_z, \sigma_z\tau_x, \tau_x, \tau_z, \tau_{xz}$. Recalling the behavior of these symmetries, we can see that only σ_{xy} generates a group without travelling waves, σ_z and $\sigma_z\tau_x$ generate groups that allow travelling waves in the x direction, $\sigma_x\tau_z$ and $\sigma_x\tau_z$ generate groups that allow travelling waves in the z direction, and the pure translations allow travelling waves in any (in-plane) direction.

Chapter 3

Numerics

On two occasions I have been asked, "Pray, Mr. Babbage, if you put into the machine wrong figures, will the right answers come out?" ... I am not able rightly to apprehend the kind of confusion of ideas that could provoke such a question.

Charles Babbage, Passages from the
Life of a Philosopher

References

- [1] Aubry, N., Holmes, P., Lumley, J. L., and Stone, E. (1988). The dynamics of coherent structures in the wall region of a turbulent boundary layer. *Journal of Fluid Mechanics*, 192:115–173.
- [2] Dauchot, O. and Vioujard, N. (2000). Phase space analysis of a dynamical model for the subcritical transition to turbulence in plane couette flow. *The European Physical Journal B-Condensed Matter and Complex Systems*, 14(2):377–381.
- [3] Daviaud, F., Hegseth, J., and Bergé, P. (1992). Subcritical transition to turbulence in plane couette flow. *Phys. Rev. Lett.*, 69:2511–2514.
- [4] Eckhardt, B., Faisst, H., Schmiegél, A., and Schneider, T. M. (2008). Dynamical systems and the transition to turbulence in linearly stable shear flows. *Philosophical Transactions of the Royal Society of London A: Mathematical, Physical and Engineering Sciences*, 366(1868):1297–1315.
- [5] Fischer, S. L. and Fischer, S. P. (1983). Mean corpuscular volume. *Archives of Internal Medicine*, 143(2):282–283.
- [6] Foias, C., Sell, G. R., and Temam, R. (1988). Inertial manifolds for nonlinear evolutionary equations. *Journal of Differential Equations*, 73(2):309–353.
- [7] Gibson, J. F. (2014). Channelflow: A spectral Navier-Stokes simulator in C++. Technical report, U. New Hampshire. Channelflow.org.
- [8] Gibson, J. F., Halcrow, J., and Cvitanović, P. (2008). Visualizing the geometry of state space in plane couette flow. *Journal of Fluid Mechanics*, 611:107–130.
- [9] Gibson, J. F., Halcrow, J., and Cvitanovic, P. (2009). Equilibrium and travelling-wave solutions of plane couette flow. *Journal of Fluid Mechanics*, 638:243–266.
- [10] Hopf, E. (1948). A mathematical example displaying features of turbulence. *Commun. Pure Appl. Math.*, 1(4):303–322.
- [11] Karman, T. v. (1930). Mechanische aenlichkeit und turbulenz. *Nachrichten von der Gesellschaft der Wissenschaften zu Gttingen, Mathematisch-Physikalische Klasse*, 1930:58–76.

-
- [12] Kawahara, G. and Kida, S. (2001). Periodic motion embedded in plane couette turbulence: regeneration cycle and burst. *J. Fluid Mech.*, 449:291–300.
 - [13] Kolmogorov, A. N. (1991). The local structure of turbulence in incompressible viscous fluid for very large reynolds numbers. *Proceedings of the Royal Society of London. Series A: Mathematical and Physical Sciences*, 434(1890):9–13.
 - [14] Lorenz, E. N. (1963). Deterministic nonperiodic flow. *Journal of the atmospheric sciences*, 20(2):130–141.
 - [15] Manneville, P. (2015). On the transition to turbulence of wall-bounded flows in general, and plane Couette flow in particular. *European Journal of Mechanics B Fluids*, 49:345–362.
 - [16] Nagata, M. (1990). Three-dimensional finite-amplitude solutions in plane couette flow: bifurcation from infinity. *J. Fluid Mech.*, 217:519–527.
 - [17] Pope, S. (2000). *Turbulent Flows*. Cambridge University Press.
 - [18] Viswanath, D. (2007). Recurrent motions within plane couette turbulence. *J. Fluid Mech.*, 580:339–358.
 - [19] Waleffe, F. (2001). Exact coherent structures in channel flow. *Journal of Fluid Mechanics*, 435:93–102.